

EUROPEAN ORGANIZATION FOR NUCLEAR RESEARCH

For internal distribution only

NP Internal Report 68.12  
1 May, 1968.

SOME REMARKS ON POSSIBLE  
IMPROVEMENTS TO THE ( $g-2$ ) EXPERIMENT

J. Bailey, H. Brechna, G. Petrucci, E. Picasso,  
P. Strolin and R.W. Williams

## CONTENTS

	<u>Page</u>
1. INTRODUCTION	1
2. PHYSICAL SIGNIFICANCE OF THE ANOMALOUS MAGNETIC MOMENT OF THE MUON	2
3. STORED MUON INTENSITY	3
4. INJECTION	4
4.1 Pion beams	5
4.2 The inflector	6
5. MEAN FIELD DETERMINATION	7
5.1 Principle of the method	7
5.2 Resolution, electrons, loss effect and magnetic scraper	11
5.2.1 Time resolution	11
5.2.2 Electrons	12
5.2.3 Loss effects and the magnetic scraper	12
6. LOSSES, ORBIT PARAMETERS, AND TOLERANCES	13
6.1 Choice of the field gradient index	15
6.2 Field and geometric tolerances	18
7. ELECTRONIC TIMING	20
8. EXAMPLES	21
9. FINAL REMARKS	24
APPENDIX I	26
APPENDIX II (by I. Pizer)	29
References	37

## 1. INTRODUCTION

The Muon Storage Ring Group has, for some months, been discussing the possibility of mounting a new experiment so as to improve, by an order of magnitude, the accuracy of the measurement of the anomalous magnetic moment of the muon.

The present error in the determination of the anomalous magnetic moment ( $a \equiv g-2/2$ ) is 300 ppm, and it is perhaps possible to reach a precision of 220 ppm with the present apparatus<sup>1,2</sup>). The goal of the new experiment is to reach an accuracy of 10-20 ppm in  $a$ , that is, about 30 times better than the present result.

We thought to introduce the following improvements into the new experiments:

- i) To increase the intensity of the muons stored in the muon storage ring.
- ii) To inject a selected pion momentum beam into the ring.

The decaying pions produce a muon beam, and this is permanently stored in the ring. The shrinking of the orbit, which is necessary to avoid the inflector, is achieved by the change of the momentum in  $\pi-\mu$  decay.

- iii) To determine with better accuracy the average radius of the muon distribution as a function of the equilibrium radii.
- iv) To reduce the instability in the muon beam. This can be achieved by a combination of more precise field shaping and a "magnetic scraper"<sup>3</sup>).
- v) To increase the product  $B \cdot Y$ .

In the past few months the following solutions have been considered:

- a) an iron magnet-yoke of 5 m diameter, 15 kG, field index  $n = 0.16$ , horizontal aperture 8 cm, vertical aperture 12 cm;
- b) an iron magnet-yoke of 10 m diameter, 15 kG, field index  $n = 0.16$ , horizontal aperture 10 cm, vertical aperture 15 cm<sup>3</sup>);
- c) a superconducting storage ring of 5 m diameter, 50 kG, field index  $n = 0.16$ , horizontal aperture 6 cm, vertical aperture 8 cm<sup>4</sup>).

Magnets (a) and (b) are of conventional design, but with the particularly severe requirements demanded by the experiment.

2. PHYSICAL SIGNIFICANCE OF THE ANOMALOUS MAGNETIC MOMENT OF THE MUON

The calculation of  $a_\mu = (g-2)/2$  depends on the following:

- (1) The dominant contribution comes from quantum electrodynamics (QED), using conventional propagator and vertex functions, and supposing that no leptons other than e and  $\mu$  exist.
- (2) There is a correction from strong interactions, both from the pion continuum and from resonances, which is calculable using spectral function techniques.
- (3) There is a correction from weak interactions, which is calculable using a W boson of some mass and magnetic moment.
- (4) There is no contribution from an unknown interaction of the muon.

Now if the experimental value for  $a_\mu$  disagrees with the theoretical values<sup>5)</sup> given by (1), with the small corrections (2) and (3), then at least one of points (1)-(4) must be wrong. The change  $\delta a/a$  has been calculated quantitatively for at least ten sub-cases:

- (1a) muon vertex modified;
- (1b,c) photon propagator modified with a mass-spectral function, or a Regge-pole factor;
- (1d) a third lepton is supposed to exist;
- (2a) contribution from  $\rho$ ,  $\omega$ , and  $\phi$  resonances;
- (2b) contribution of the time-like  $\pi$  form-factor;
- (3a) contribution of a W boson of reasonable magnetic moment;
- (4a,b,c) a scalar, pseudoscalar, or vector field interacts with  $\mu$ .

The converse does not hold -- some of these effects may exist, but do not change  $a_\mu$ , because of cancellation (however, this would be a striking property of nature, akin to CVC!). Any advance in knowledge will come by combining the (g-2) experiment (which is very precise but measures only one number) with other experiments.

### 3. STORED MUON INTENSITY

The muon capture yield per available proton of given energy will be a function of the method of injection, and of the ring parameters, that is: (1) aperture of the storage region ( $b$  in the horizontal plane,  $a$  in the vertical one); (2) radius of the ring ( $\rho$ ); (3) magnetic field ( $B$ ); (4) field index ( $n$ ). It is difficult to express all these parameters in a general formula. However, for a given injection system and inside a limited range of the parameters, one can accept the following expression:

$$P_{\mu} = f \cdot \frac{ab^3}{\rho^4} n^{1/2} (1-n)^{5/2} \cdot p_{\pi} \quad Y = f_1 \frac{ab^3}{\rho^3} n^{1/2} (1-n)^{5/2} B \cdot Y,$$

where  $P_{\mu}$  is the muon capture yield,  $Y$  is the yield of pion production (per GeV/c and steradian) which is a function of the proton and the pion momenta, and  $f$  or  $f_1$  are factors depending on the chosen injection system.

The formula can be explained simply as the product of the angular acceptance in the vertical plane  $[(a/\rho)n^{1/2}]$ , the angular acceptance in the horizontal plane  $[(b/\rho)(1-n)^{1/2}]$ , the momentum bite of the pions  $[(b/\rho)p_{\pi}(1-n)]$ , and finally the acceptable fraction of the muon momentum spectrum  $[\sim (b/\rho)(1-n)]$ .

In  $f, f_1$  the decay probability of the pions must be included. This probability is very high in the case of injection of protons in the ring onto an internal target; it is lower in the case of pion injection through an inflector; and it is very low in the case of backward decay trapping. In  $f, f_1$  the losses due to the decay angles must also be included. These losses might be rather high when the angular acceptances of the ring are comparable to the decay angles. Finally, in the particular case of pion injection, the matching factor must also be included in  $f, f_1$ ; it will result depending on the ring parameters, but subject to practical limitations in the maximum possible beam acceptance at each chosen pion momentum.

#### 4. INJECTION

Three methods are available in order to trap muons in the storage region of the ring:

- i) by injecting protons in the ring and having them interact with a target located at the limit of the storage region;
- ii) by directly injecting muons of the desired momentum and putting them in stable orbits by means of a very fast inflector;
- iii) by injecting pions of chosen momentum so that their chance to produce trapped muons is high.

The first method is being used in the present g-2 experiment. The pions with the right momentum, produced in the internal target are traveling around the ring for nearly three revolutions before hitting the target again; most of them will decay before, so that the trapping efficiency for circulating pions is rather high. However, a great number of pions with wrong momenta will also travel long enough inside the ring, and will produce a considerable number of muons which will be trapped but which will have a wrong polarization; furthermore, by injecting the protons, the general background is very high around the target, and the electron counters can be located only at the opposite side of the ring.

The second method presents great technical difficulties. In fact, the inflector to trap the muons in a stable orbit must be switched off in a time shorter than the revolution time of the particle in the ring (50 nsec for a 5 m diameter magnet); the lack of straight section, due to the need for a field which is as homogeneous as possible, also increases the difficulty of building such an inflector.

The third method looks the most convenient. The pion beam produced from an external target must, of course, be matched so as to exploit, to a large extent, the acceptance of the ring. The problems presented by the inflector are not too difficult, and it will look like a coaxial line excited with pulses of a few microseconds. The background will be reduced considerably with respect to the first case, so that the counters could be located all along the ring. The polarization of the muon will be very

high, since most of the muons will be produced by pions of nearly the same momentum; furthermore the electrons existing in the pion beam might easily be eliminated before reaching the ring. A disadvantage of this method lies in the rather short path (less than one revolution) that the pions will run inside the ring before leaving the storage region. The trapping efficiency per circulating pion is thus lower than in the internal target method; however, the number of trapped muons might be the same since the matching procedure will compensate the lower trapping efficiency.

A possible version of this last method is to inject pions with momentum equal to about 1.72 times the described muon momentum, with the purpose of trapping the muons emitted backward in the c.m. system of the pions. This system looks attractive at first sight because it does not require any inflector: the pion beam will enter the storage area and cross it, leaving the ring through an opening; hence the background will be very small. However, the trapping efficiency for circulating pions will, in this case, be very small due to the very short path of the pions inside the chamber: the degree of polarization might also not be as high as in the previous case. This method could thus be adopted only by using a very strong pion beam. The construction of the magnet will, in this case, be particularly simple.

#### 4.1 Pion beams

If pion injection is adopted, a beam has to be provided between the target and the ring. The beam will select the desired momentum, reduce the background, and match the ring acceptance. A possible layout is shown in Fig. 1, and the optical behaviour in Fig. 2.

Since we envisage using protons extracted from the proton synchrotron, it is possible to start the beam at  $0^\circ$  production.

The beam consists of two focusing stages. At the end of the first one a double focus is obtained, and in this position, where the momentum slit is also located, a heavy plate of a few millimetres thickness might be mounted in order to eliminate the electron contamination. The pion losses in the plate would be lower than 10-20%.

The angular acceptance of the beam, designed for a maximum momentum of 2.2 GeV/c, is  $\pm 13$  mrad in the horizontal plane and  $\pm 40$  mrad in the vertical plane. The emittance at the entrance to the storage ring will be of the order of 800 mm mrad in the vertical plane and 120 mm mrad in the horizontal plane; these values are inclusive of chromatic aberrations for a momentum bite ( $\Delta p/p$ ) of  $\pm 0.6\%$ , and of the scattering introduced by the plate foreseen for the electron absorptions. The sizes of the target would be 3 mm in the horizontal and 5 mm in the vertical planes. The second stage of the beam provides compensation of the momentum dispersion and matches the ring acceptance. The beam size at the inflector will therefore be about 12 mm in the horizontal plane and 60 mm in the vertical plane, with a total angular divergence of 10 mrad in the horizontal plane and 13 mrad in the vertical plane.

#### 4.2 The inflector

The inflector might consist of a coaxial line closed at its end. Figure 3 shows a possible cross-section of this line and a possible layout of the inflector inside a 10 m ring.

Tentative parameters of the inflector could be:

magnetic induction	6 kG
length	2.5 m
useful aperture	{ 15 mm in the horizontal plane 80 mm in the vertical plane.

Such an inflector would, for instance, deviate 2.2 GeV/c particles by about 200 mrad. The distance between the last quadrupole of the beam and the exit from the inflector in the storage region of the ring might be of the order of 5 metres (for a 10-metre conventional ring).

The pulse to excite the inflector might be a simple sinusoidal one obtained by discharging a condenser bank; there is no need for a very short pulse, because negligible field will be produced outside the line; on the other hand, the pulse should not be too long in order to limit the effect of the electromagnetic forces.

With a 5  $\mu$ sec pulse (half sine wave) and 6 kG maximum field, the capacity needed is 20  $\mu$ F charged at about 12 kV. The peak current will amount to about 110,000 A, and the stored energy to about 1400 J.



## 5. MEAN FIELD DETERMINATION

### 5.1 Principle of the method

The value obtained for the anomalous moment is directly proportional to the mean value of magnetic field experienced by the muons (apart from a small correction for vertical oscillations). To obtain the mean field, and given the gradient necessary for trapping the muons, we have to know something about the equilibrium radii of the muons. We might consider the following:

a) A small horizontal aperture. With a gradient of  $n$ -value 0.16, a spread in field of  $\pm 10$  ppm would mean a full width of  $1.25 \times 10^{-4}$  radius (R), or 0.3 mm. The intensity would be negligibly small.

b) An accelerating cavity which would impose a mean energy, and therefore a mean field on all particles, as suggested by Orlov<sup>6</sup>). We have not studied this in detail, but the engineering problems of introducing a very-high-field RF electrode into the storage ring seem formidable. In addition, if the particles experience even a very small radial electric field which does not average to zero, their precession rate will be altered. These difficulties have discouraged us from pursuing this method.

c) The method used in the present experiment. The particles are injected into the storage ring by (essentially) one RF bunch from the PS, which has a time-spread of about 10 nsec. Since the period of a trapped particle in the ring is about 52.5 nsec, the rate of muon decay electrons as seen by a single counter has a "fast-rotation" modulation of this period. The assumed distribution of muon orbits is then adjusted to fit the observed modulation. We have studied this method extensively in the present ring, both with real data and with artificial (Monte Carlo) data. The results are sensitive to the effective width of the injection pulse (which is not well known in practice) and to the non-rotating background which is always present. It seems that we could assign a standard deviation of 2 mm to the mean radius as it is now determined (corresponding to 100 ppm in  $g-2$ ), but higher statistical precision does not lead to a smaller error.

Part of the difficulty with the present determination is caused by the injection of the proton beam into the ring. The counting system does not recover from this very large overload until about  $1.2 \mu\text{sec}$  after injection. By this time the muons on small radii have overtaken the tail of the large-radii muons, so that the modulation is only indirectly related to the mean radius. The fitting process takes this into account, but we have to rely on Monte Carlo studies to estimate its accuracy. This difficulty should disappear in the new project in which pions, rather than protons, would be injected. One can then observe the sample before it begins to overlap itself.

Proton injection is presumably also responsible for the non-rotating background we observe, so again pion injection should improve the fast-rotation analysis.

It is possible that in these circumstances the fitting programme would give very accurate results for sufficiently large samples of data, perhaps a few tenths of a millimetre, provided the pulse-width problem can be solved. The present Monte Carlo studies are not accurate enough to answer this question.

In order to use the mean field determined from early times in connection with the precession frequency measured hundreds of turns later, we must be sure that the muon sample does not undergo selective loss which would depopulate its non-uniformity. A discussion of losses will be found in Section 6.2. Table 1 indicates the uncertainty introduced by losses; for instance, a 1% loss, if it occurs at one side of the storage region, will cause a shift in mean field by about 13 ppm. To avoid this, one might artificially introduce a modulation in the sample during the  $g-2$  observation time. This scheme is considered in the appendix of Ref. 3. It appears to be technically very difficult, and perhaps not sufficiently accurate.

d) The method we propose for a new experiment is a variation of method (c) in which the rotational structure is observed before the sample overlaps itself. In this case there is a clearly-defined mean rotation time  $T$ , which can be obtained without knowing the injection time  $t_0$  or the injection pulse width. Provided there is no non-rotating background (so

Table 1

Relative error in  $g-2$  caused by a loss at one edge of the storage region of a fraction  $F$  of the population, and the consequent shift of mean radius. A triangular distribution of equilibrium radii is assumed to be truncated by a fraction  $\chi$  of its half-width. The error is tabulated in parts per million, and for a given loss is nearly the same for the superconducting ring or the iron ring. However, the former has 3.3 times more turns per lifetime.

F = fraction of muons lost	0.0018	0.005	0.011	0.125
X = fraction of half-aperture from which muons are lost	0.06	0.1	0.15	0.5
Resulting error in ppm	4	9	13	180

Table 2

Fast rotation mean-field analysis; comparison of the 5-metre superconductor ring with a 10-metre iron ring

	Supercond.	10 m iron
$\nu$ = number of turns before overlap, assuming 15 nsec injection pulse.	30	43
Time for 3 turns of pions.	0.16 $\mu$ sec	0.32 $\mu$ sec
Time for magnetic scraper	1 $\mu$ sec	2 $\mu$ sec
$\nu_c$ = number of turns to beginning of fast-rotation analysis.	22	22
$\sigma_R$ = r.m.s. spread of muon orbits.	1.2 cm	2 cm
$y = \nu/\nu_c$	1.365	2
$\sigma_{T/T}$ = relative error in mean rotation time.	$0.06/\sqrt{N}$	$0.02\sqrt{N}$
$\sigma_{T/T}$ in terms of the total numbers of muons observed at all times, $N_T$	$0.78/\sqrt{N_T}$	$0.09/\sqrt{N_T}$
$\sigma_{a/a}$ = relative error in $g-2$ from mean field, $n\sigma_{T/T}$ , assuming $N_T = 10^8$	13 ppm	1.6 ppm

that the bunches of counts are distinct for the period of observation) the method is straightforward: the mean time of each bunch is determined from the data, and the mean times are least-squares fitted to a straight line. The details have been worked out in an internal memo<sup>3</sup>). The advantage of the method is clarity -- one can see at once from the number of counts, etc., what the expected error is.

To estimate the accuracy afforded, we can use the approximate formula given in Ref. 3 for observation from turn  $\nu_c$  to turn  $\nu$ , with observed number of counts  $N$ . The mean rotation time  $T$  can then be determined with a relative error

$$\frac{\sigma_T}{T} = \frac{\sigma_R/\bar{R}}{\sqrt{N} \sqrt{1 - y \left( \frac{\ln y}{y - 1} \right)^2}},$$

where  $\sigma_R$  is the r.m.s. spread in equilibrium radii around the average  $\bar{R}$  and  $y = \nu/\nu_c$ .  $\sigma_R$  is roughly one-fifth of the full width of the trapping region  $\Delta R$ . The beginning of the observation period is determined by the time at which the muon population becomes stable, which is discussed below. The end of the period cannot be later than the time at which the muon bunch begins to overlap itself, which is approximately

$$t = \frac{R}{\Delta R} (T - \text{pulse width}) .$$

Table 2 gives some typical results for the superconducting ring, with parameters as given in Section 1, and for comparison the same quantities for a 10 metre iron ring as discussed in Ref. 3. Note that the iron ring parameters have been chosen essentially to optimize the accuracy of the fast-rotation analysis, while the superconducting ring is weighted more heavily on the side of accuracy of the precession frequency.

We would in any case determine the (approximate) shape of the distribution of equilibrium radii, as in method (c), since in principle it is needed in order to go from the mean rotation time to the mean field.

## 5.2 Resolution, electrons, loss effect and magnetic scraper

The extremely optimistic picture printed above for the accuracy of the mean field depends on obtaining at very early times a stable, background-free sample of muons, and on a sufficient accuracy in measuring their decay time. We think these conditions can be met. Some of the relevant points are as follows:

### 5.2.1 Time resolution

The digitron principle, as now used, is based on a free-running crystal clock and should be sufficiently accurate -- tests can ascertain the kind of time-dependent baseline shifts, etc., which may be present. However, it has a least count of  $\tau$  (at present 5 nsec) and we want each value of the mean time to a precision of perhaps 50 psec. Fortunately the various timing signals (arrival of the beam, arrival of a muon decay electron) are completely random with respect to the clock phase. A simple analysis shows that repeated observation of a pair of signals, separated by a time  $n\tau + \delta$  ( $\delta < \tau$ ) gives an unbiased estimate of  $n\tau + \delta$  with a standard deviation  $\sqrt{\delta(\tau - \delta)}/N$ , where  $N$  is the number of pairs of counts. Averaging this over a distribution of times which is wide compared to  $\tau$  gives the standard deviation in the mean time  $\bar{t}$  due to this effect. The result is  $\sigma_{\bar{t}} = \tau/\sqrt{6 N_T}$ , whose  $N_T$  is the total number of pairs of counts, that is the number of counts in each bunch. This can be compared with the error caused by the natural spread<sup>3)</sup> in the bunch  $\sigma_\alpha$ , which is  $\sigma_\alpha/\sqrt{N_T}$ , so the ratio of time-resolution error to natural-spread error is

$$\frac{\tau}{\sigma_\alpha \sqrt{6}} .$$

Now  $\sigma_\alpha$  is typically 3 nsec for the beginning of the observation period, and 6 nsec at the end, so this ratio is less than 1 even for a 5 nsec least count; a 2.5 nsec count would be safer but not absolutely essential.

### 5.2.2 Electrons

In the superconducting ring, electrons lose energy so rapidly that they are lost before the fast-rotation period starts. In the iron ring, the electrons lose 1.2 mm per turn, and are present in the fast-rotation period. A fraction  $f$  of electrons with mean radius differing by  $\Delta R$  from that of the muon will cause an error in radius  $f \Delta R$ . Since  $\Delta R$  can be of the order of a centimetre, this poses a severe restriction on the iron ring; it constitutes a clear advantage of the superconductor. With the iron ring one would have to clean the pion beam of electrons to whatever extent possible, and then rely on a system of scrapers in the storage ring, somewhat like the present system.

Alternatively, one could lengthen the period of observation of the fast rotation, either by reducing the horizontal aperture (with loss of intensity) or by going back to method (c), fitting the late-time modulation.

### 5.2.3 Loss effects and the magnetic scraper

As illustrated in Table 2, a particle loss of 0.5%, if it occurs at one edge of the equilibrium-radius distribution, corresponds to 9 ppm error in mean field and therefore becomes significant when the fast-rotation method is used. The muon sample is defined by the physical aperture of the storage region. This is not completely uniform with respect to the closed orbits of the muons, so that many betatron oscillations (tens or even hundreds in certain cases) are required to define the sample perfectly. Deviations from an ideal field will cause a slow build-up of betatron oscillations (see Section 6) so that losses continue to occur, at a rate which should be low, throughout the entire history of the muon sample. To obviate this it has been proposed<sup>3)</sup> to displace the entire muon sample adiabatically by perhaps 10% of the aperture dimensions, thus deliberately removing the muons in the outer part of the aperture, and, when the displacement is restored, leaving a sample well within the allowed storage region. Such a device has been called a magnetic scraper.

A way of achieving this is discussed in Ref. 3, where it is shown that a magnetic field of the order of 100 gauss (or 30 gauss for

an iron ring) will have the desired effect. It is also shown that the displacement will be reasonably adiabatic if it is a single, full sine wave of period at least twenty times the rotation period of the muons. Since one has to finish this sample-stabilizing before starting the fast rotation analysis, one makes it as short as possible -- one microsecond in the case of the superconducting ring. The field is applied by single-turn coils near the storage volume. The arrangement necessary for the superconductor is discussed in Ref. 4, where it is shown that the voltage required, whilst high, is not unfeasible.

In the iron magnet, and to a lesser extent in the superconductor, there will be eddy-current effects in the nearby conducting surfaces. These act like image currents, reducing the field and changing its direction while the pulse is applied. In a typical case (iron magnet) the field is reduced 20% and shifted 2° in the centre of the storage region.

There is some flux penetration during the pulse, which means that the eddy-currents persist after the current in the coils is cut off. An exact calculation of a very simple case indicates that the field due to these persistent currents lasts for 5 or 6 times the length of the pulse, and has a maximum amplitude about 10% of the amplitude of the image-current field (the fact that the pulse is symmetrical cancels out most of the effect). Thus we have present for several microseconds about  $0.2 \times 0.1$ , or 2%, of the scraper field.

It is clear that the requirement of keeping the eddy-currents down will put some rather awkward constraints on the design of the walls of the storage region, etc.

## 6. LOSSES, ORBIT PARAMETERS, AND TOLERANCES

The requirements on particle losses imposed by the (g-2) experiment are quite severe. We justify these requirements if we take into account that the average radius determination will be done by measuring the rotational structure before the sample overlaps itself. Therefore losses cause error in the measurement of the average radius; in fact, if we lose particles in the interval of time in which we measure the revolution period, the average radius may be different from the radius appropriate to the interval of time in which we measure the  $\omega_{g-2}$  quantity.

Another source of error due to the losses causes a progressive phase shift in the angular velocity  $\omega_{g-2}$ . A radially selective loss will change the phase of  $\omega_{g-2}$ . This source of error has been discussed in detail by Williams<sup>3)</sup>. If there should be a correlation between the polarization and the equilibrium radii, and if during the period in which we determine the  $\omega_{g-2}$  we lose muons, then the direction of the mean polarization of the sample would change. This will depend on the shape of the muon distribution versus equilibrium radii, and on whether we lose particles in symmetric way or not. Of course, if the sample will be totally longitudinally polarized, the losses will not introduce any progressive phase-shift effect. In the new project, using the pion injection system, we hope to produce a sample of muons with an average value of the longitudinal polarization of 95%. The dependence of the polarization versus equilibrium orbit will be around 5%.

In Table 3 we quote the relative error in  $(g-2)$ , in part per million, from progressive phase shift caused by a loss at one edge of a fraction F of the muon population for various values of mean polarization  $\bar{P}$  and correlation fraction  $\epsilon$ . The fraction F is per mean lifetime.

Table 3

F →	0.0018	0.0050	0.011	0.125	0.245	0.362	0.5
$\bar{P} = 0.95$ $\epsilon = 0.5$	4	10	22	250	500	730	1000
$\bar{P} = 0.95$ $\epsilon = 0.1$	1	2	4	50	100	150	200
$\bar{P} = 0.95$ $\epsilon = 0.05$	0.5	1	2	25	50	75	100

From the table it can also be seen that if the fraction of the sample which is correlated with the equilibrium radii is 5%, we cannot tolerate more than 5% losses in order to determine  $(g-2)$  better than 10 ppm. The dependence of the relative error in  $(g-2)$  as function of  $\bar{P}$  is given in Ref. 3.

More severe requirements are imposed by the determination of the mean radius (see Section 5); we hope to lose less than 0.5% of the particles by doing a more precise field shaping and using a "magnetic scraper"<sup>3)</sup>.



The orbit parameters of the possible muon storage ring must satisfy the following two special requirements:

- i) the magnetic field gradient must be relatively small in order to allow a precise determination of the average magnetic field acting on the muons;
- ii) particularly severe limitations are imposed on particle losses.

The first of these requirements leads to a design which is unusual for constant gradient synchrotron accelerators, the most relevant feature of such a design being the large vertical aperture. Due to the second requirement, particular attention has to be paid to the choice of orbit parameters, so that "resonances" which may cause particle loss are avoided as much as possible. In Section 6.1 we discuss the choice of a magnetic field gradient index and its tolerance, in order to satisfy the above two requirements. This is independent of the particular solution adopted for the new muon storage ring.

In Section 6.2 the tolerances to be imposed on the magnetic field itself and on the geometry of the ring are worked out in such a way that the equilibrium orbits are not excessively displaced from their ideal positions. A theoretical computation of these tolerances is carried out for the superconducting muon storage ring. The distortions of the equilibrium orbits which can be expected in the two proposed conventional magnets are worked out by scaling those obtained in the present muon storage ring.

### 6.1 Choice of the field gradient index

Denoting by  $B$  the vertical component of the magnetic field at the radius  $\rho$ , the field gradient index  $n$  is defined as:

$$n = - (\rho/B)(\partial B/\partial \rho) . \quad (1)$$

The particles perform stable betatron oscillations about their equilibrium orbits, if on these orbits

$$0 < n < 1 . \quad (2)$$

The number of betatron oscillations per revolution in the radial and in the vertical plane are  $Q_x$  and  $Q_z$ , respectively, expressed by

$$Q_x = \sqrt{1-n} ; \quad Q_z = \sqrt{n} . \quad (3)$$

In practice, the field gradient index which characterizes the properties of the linear particle motion about the equilibrium orbit is not constant over all the aperture, because of field imperfections. Hence, as shown by Eq. (3), in the plane  $Q_x, Q_z$  the working points cover an arc of finite length on the circle of unit radius centred at point  $Q_x = 0, Q_z = 0$ .

If the working point is close to resonance lines, defined in the  $Q_x, Q_z$  plane by

$$a Q_x + b Q_z = k, \quad (4)$$

where  $a, b,$  and  $k$  are integers, the  $k^{\text{th}}$  harmonic of the azimuthal distribution of derivatives of order  $(|a| + |b| - 1)$  of magnetic field imperfections may excite a resonant growth of oscillation amplitudes, thus causing particle loss. As a consequence, periodicities of this order must be avoided in the design. The quantity  $|a| + |b|$  is called the order of the resonance and is denoted by  $m$ . In the case where  $m \leq 2$ , linear field imperfections may cause instability of the particle motion. Consequently, such resonances are called linear resonances. Non-linear resonances are related to non-linear field imperfections, and occur for  $m > 2$ . They may cause instabilities even when in the linear approximation the particle is stable. Resonances are called sum resonances if  $a$  and  $b$  have the same sign, otherwise they are called difference resonances. Because of the severe requirements imposed on particle losses by the g-2 experiment, particular attention has to be paid in order to avoid that the arc, where working points lie, should cross resonance lines.

The general theory of linear and non-linear resonances is given in the papers by Schoch<sup>7)</sup> and Hagedorn<sup>8)</sup>. Difference resonances lead only to coupling between the two transverse oscillation modes. The consequent transfer between them of oscillation energy may cause particle loss if the aperture limitations are more severe for one of the two. Therefore, difference resonances should, as far as possible, be avoided in the muon storage ring. Sum resonances lead to transfer of energy from the longitudinal motion to the transverse motion and may cause a large increase of amplitudes of transverse oscillations, an indefinite

growth of amplitudes being limited by non-linearities which move betatron frequencies out of tune with the driving force as the amplitude increases. Resonances become less dangerous as the order becomes higher. Resonances of order higher than four are in general stable for sufficiently small amplitudes, because of detuning effects as oscillation amplitudes increase.

As discussed above, the field gradient index has to be particularly low in comparison with the values usually adopted. The lower limit is given by the presence of the linear resonance lines  $Q_x = 1$  and  $Q_z = 0$ . Approaching these lines, set-up errors cause large distortions of equilibrium orbits and large displacements of betatron oscillations. Figure 4 shows the resonance lines up to the fifth order in the region of the  $Q_x, Q_z$  plane, where the nominal working point could be located. Crossings of the working circle with resonance lines are labelled with the corresponding value of  $n$ . The nominal  $n$ -value has to be chosen in such a way that, taking into account the spread of  $n$ -values caused by field imperfections, a minimum number of resonance lines is crossed.

A spread of  $\pm 15\%$  on the  $n$ -values will be assumed. Between the crossings with the fourth-order sum resonance line  $Q_x + 3Q_z = 1$  and with the third order difference resonance line  $Q_x - 2Q_z = 0$  (the so-called Walkinshaw resonance), there is an interval that is free from crossings with sum resonance lines of order smaller than five, and from difference resonance lines of order smaller than four. This region corresponds to  $n$ -values ranging from  $n = 0.1261$  to  $n = 0.2$ . The nominal  $n$ -value could be  $n = 0.16$ , which is approximately at the mid-point of this interval. The spread on  $n$ -values corresponding to the full length of the interval is  $\pm 2\%$ .

Although the resonance lines that are crossed should not lead to an indefinite increase of oscillation amplitudes, they could cause beat oscillations of these amplitudes. In this connection a magnetic scraper (as discussed in Ref. 3) would be convenient, since it would provide a free space between the circulating muon beam and the enclosure walls, where a certain amount of these beat oscillations can take place without causing any particle loss. Moreover, since even unstable particles (which are going to be lost) take a certain time to cross this region, instabilities with slow growth-rate become unimportant for the experiment.

The performance of the muon storage rings could, as far as particle losses are concerned, be pushed to its intrinsic limits if one could have the possibility of changing the field gradient index. For example, one can see from Fig. 4 that in the interval limited by the crossings with the resonance lines  $2Q_x - 2Q_z = 1$  and  $Q_x - 2Q_z = 0$ , no resonance line of order smaller than six is crossed. If the spread on the  $n$ -values turns out to be smaller than that corresponding to this interval ( $\pm 8.3\%$ ) it will be convenient to shift the  $n$ -value to the mid-point of this interval ( $n = 0.184$ ). This operational flexibility is a feature of the superconducting muon storage ring, where the field gradient is given by a quadrupole coil. This coil can be powered at different current levels, independently from the current in the main dipole coil which provides the main bending field. In a conventional magnet, a similar flexibility requires the use of pole-face windings.

## 6.2 Field and geometric tolerances

In order to avoid excessive displacements of the equilibrium orbits in the superconducting muon storage ring, the requirements which must be met by the accuracies in the magnetic field and in the positioning of the magnet will first be worked out.

As described in the paper by Green and Courant<sup>9</sup>), a convenient formulation of the problem is in terms of Fourier components. The azimuthal variation of the vertical magnetic field  $B$  is expressed by the Fourier series:

$$B(\vartheta) = B_0 \left[ 1 + \sum_k a_k \cos (k\vartheta + \delta_k) \right], \quad (5)$$

where  $\vartheta$  is the azimuthal angle,  $B_0$  is the nominal vertical magnetic field, and  $\delta_k$  is a phase constant. The harmonic  $a_k$  of the relative error on the vertical magnetic field produces a  $k^{\text{th}}$  harmonic of distortions of the equilibrium orbit in the radial direction, the amplitude of which is

$$x_k = \frac{a_k \rho}{k^2 + n - 1} \quad (6)$$

The  $k^{\text{th}}$  harmonic  $\Delta\rho_k$  of radial displacements of the magnet is equivalent to an harmonic  $a_k = n \Delta\rho_k / \rho$  of relative errors on the vertical magnet field. Hence it gives a radial distortion of the equilibrium orbits having amplitude

$$x_k = \frac{n\Delta\rho_k}{k^2 + n - 1} . \quad (7)$$

An equation similar to Eq. (7), with the substitution of  $n$  to  $(1-n)$ , gives the amplitude  $z_k$  of the distortion of the equilibrium orbits in the vertical direction caused by the harmonic  $\Delta z_k$  of vertical displacements:

$$z_k = \frac{n\Delta z_k}{k^2 - n} . \quad (8)$$

Tilts of the median plane of the magnetic field, with a  $k^{\text{th}}$  harmonic  $\alpha_k$  of the tilting angle, are equivalent to vertical displacements of the magnet by  $z_k = \rho \alpha_k / n$ . Hence they give

$$z_k = \frac{\rho \alpha_k}{k^2 - n} . \quad (9)$$

Equations (6), (7), (8), and (9) show that first harmonics of set-up errors have a predominant effect. The superconducting muon storage ring will be provided with a certain number of dipole correcting coils (each covering a section of the ring circumference) for azimuthal corrections of set-up errors causing radial closed-orbit distortions. Taking as values of the first harmonics

$$a_1 = 3 \times 10^4$$

$$\Delta\rho_1 = 1 \text{ mm}$$

$$\Delta z_1 = 1 \text{ mm}$$

$$\alpha_1 = 1 \text{ mrad} ,$$

and adding quadratically the contributions to equilibrium orbit distortions in each plane, one obtains a total distortion of the equilibrium orbit of  $\pm 5.2$  mm in the radial plane and of  $\pm 4$  mm in the vertical plane, as shown in Table 4 where the influence of higher order harmonics has been taken into account. One can remark that because of the low field-gradient index adopted, the influence of geometrical set-up errors is relatively small.

Table 4

Extreme displacements of equilibrium orbits  
in the superconducting storage ring

	Assumed error	Extreme displacement
<u>Radial</u>		
Relative magnetic field error	$3 \times 10^{-4}$	$\pm 5.0$ mm
Radial magnet displacements	1 mm	$\pm 1.1$ mm
Total extreme displacements of equilibrium orbits		$\pm 5.2$ mm
<u>Vertical</u>		
Tilts of the median plane	1 mrad	$\pm 3.9$ mm
Vertical magnet displacements	1 mm	$\pm 0.2$ mm
Total extreme displacements of equilibrium orbits		$\pm 4.0$

The case of a conventional magnet will now be considered. Equations (6) to (9) show that closed orbit displacements are proportional to the radius of the ring if the errors  $a_k$ ,  $\Delta\rho_k/\rho$ ,  $\Delta z_k/\rho$ , and  $\alpha_k$  are taken constant. Equilibrium orbit distortions are known only in the radial plane for the present muon storage ring, and amount to  $\sim \pm 3$  mm. Equilibrium orbit distortions of the same order of magnitude are supposed to occur for vertical motion. Similar distortions should be obtained from the 5 m, 15 kG magnet, assuming the same relative set-up errors, whilst twice as much should occur in the 10 m, 15 kG magnet.

## 7. ELECTRONIC TIMING

Preliminary estimates indicate that by using about five ejected proton bunches we may have of the order of 1000 "events" (observed electrons from muon decay) in every 1-second cycle of the PS. These events are distributed with an exponential decay-time of  $\sim 50$   $\mu$ sec over a time interval of about 300  $\mu$ sec, starting at "injection time" given either by a pick-up signal from the protons or a thin scintillator in the pion beam. We must record the arrival time of each event with great ( $\leq 5$  nsec) accuracy during the first  $\sim 6$   $\mu$ sec, and lesser accuracy ( $\leq 40$  nsec) thereafter. A possible digitron design sketched by Pizer (see Appendix II)

uses two sets of 32 fast (200 MHz) 8-bit scalers, each set recording alternately and then dumping into a fast buffer store while the other set is recording. (In the recording period of  $1.28 \mu\text{sec}$  we expect  $\sim 25$  events.) The fast buffer store of 1000 8-bit words would transfer into a fast computer after each muon storage cycle. Other possibilities, such as (a) the use of 25 MHz scalers, or (b) repetition of the ejection-recording-transfer cycle (which takes a few msec) several times per PS cycle (if kicker power supplies are adequate), or (c) recording data only in two or three small sections of the  $300 \mu\text{sec}$  interval, may greatly reduce the scaler and memory capacity required.

## 8. EXAMPLES

We have considered the following solutions:

- 1) A ring of 5 m diameter, 15 kG,  $n = 0.16$ ,  $\Delta n/n = \pm 15\%$ , horizontal aperture 8 cm, vertical aperture 12 cm with pion injection. The improvements with respect to the present storage ring are:
  - i) less background; and therefore more accurate determination of the average radius;
  - ii) higher value of the initial longitudinal polarization;
  - iii) larger acceptance, therefore high intensity stored;
  - iv) a more accurate choice of the parameters in order to minimize particle losses.
- 2) The 10 m diameter iron ring was studied in some detail by one of the authors (R.W.W.)<sup>3)</sup>. The parameters are essentially as follows:

10 m diameter, 15 kG,  $n = 0.16$ ,  $\Delta n/n = \pm 15\%$ , horizontal aperture 10 cm, vertical aperture 15 cm. Injection of pions. The momentum of the stored muons will be  $p_\mu = 2.17 \text{ GeV}/c$  with a  $(\Delta p/p)_\mu = 0.8\%$ .

The advantages mentioned under point (1) are still valid. Other advantages are the more accurate determination of the average radius (see Section 5) and the longer lifetime. This longer time-base improves the statistical precision of the fit to  $\omega_{g-2}$  and reduces the influence of

systematic errors. The muon lifetime will be lengthened by a time-dilation factor  $\gamma \sim 20$  to a theoretical value of  $\sim 45 \mu\text{sec}$ . This allows the precession to be followed out to times of the order of 200-300  $\mu\text{sec}$  compared to the 100-150  $\mu\text{sec}$  of the present experiment. The predicted intensity, using the forward decay scheme, gives 610 stored muons per radio-frequency bunch. This value has been obtained using the method described in Appendix I. This calculation was based on the following assumptions

Number of protons per RF bunch	$5 \times 10^{10}$
Target efficiency	0.4
Momentum of the proton beam	20 GeV/c
Yield of the pion beam of 2.17 GeV/c	1.3 pions/GeV/c · sr · interacting proton
Flux of the pion beam injected in the muon storage ring	$2.6 \times 10^5$

The rate of the decay electrons of energy greater than  $\frac{1}{2} E_{\text{max}}$  will be around 6 times higher than the present rate. If we consider the fact that we will have counters all the way around the ring ( $\times 4$  more than now), and that the aperture shape is more favourable for detecting decay electrons than in the present ring, we will expect a rate which should be around 40 times higher than in the present experiment. The CPS cycling rate will be a factor of two higher; therefore a sample of  $10^8$  decay electrons of energy greater than  $\frac{1}{2} E_{\text{max}}$  will be obtained in about 3 weeks of good data taking if we use three bunches per CPS cycle. The higher intensity will permit us to do a diagnostic faster than in the present experiment. To determine the accuracy, we use the approximate formula derived by Goddard, which agrees well with the error found by the FIT 62 program:

$$\sigma_{\omega} = \frac{\sqrt{2}}{\gamma \tau_0 A \sqrt{N}} .$$



With  $10^8$  analysed decay electrons and a value of the asymmetry parameter  $A = 30\%$ , we will get an accuracy  $\sigma_{\omega/\omega} = 8$  ppm. The relative error in  $(g-2)$  from mean field assuming  $N = 10^8$  is  $\sigma_a/a = 1.6$  ppm. Figure 5 shows the trapping efficiency versus  $\Delta p/p$  of the pions, and Fig. 6 shows the momentum spectrum of the stored muons.

- 3) We were interested in studying the possibility of using a higher field. In the present experiment we can follow the precession cycle of the angle  $\vartheta$  of the spin relative to the muon momentum ( $\vartheta = a \omega_0 Bt$ ) to times of the order of  $100 \mu\text{sec}$  or more ( $\sim 30$  precession cycles) compared to the  $\sim 4 \mu\text{sec}$  of the earlier experiment<sup>10)</sup>. In both experiments the field is close to  $\sim 17$  kG.

In the 10 m diameter ring the Lorentz factor  $\gamma = (1 - \beta^2)^{-1/2}$  will be  $\sim 20$ . Another possibility is to increase not only the storage time but also the field ( $\omega_{g-2} = a \omega_0 \bar{B}$ ).

Thus we investigated the possibility of constructing a storage ring of 5 m diameter with a central field of 50 kG. The horizontal aperture is 6 cm and the vertical aperture is 8 cm. The field index is  $n = 0.16$  and  $\Delta n/n = \pm 15\%$ .

Such a superconducting storage ring was investigated in detail by some of the authors<sup>4)</sup>.

Here we will report only the conclusions of our study of the advantages that such a field would present with respect to the  $(g-2)$  measurement. Let us note that the parameters of the superconducting ring have been chosen to optimize the accuracy of the precession frequency.

We used the approximate Goddard's formula to compute the relative error in  $\omega_{g-2}$ ;

$$\frac{\sigma_{\omega_{g-2}}}{\omega_{g-2}} = \frac{\sqrt{2}}{A\sqrt{N}} \frac{m_0^2 c^3}{\tau_0 a e^2} \frac{1}{RB^2} .$$

Note that in any injection mechanism in which the pions are not truly trapped, a higher field leads to a smaller decay fraction, so that the accuracy in  $\omega_{g-2}$  improves as  $B^{2/3}$  rather than  $B^2$ .

Assuming  $N = 10^8$  analysed decay electrons, and a value of the asymmetry parameter  $A = 30\%$ , the relative error in  $\omega_{g-2}$  is

$$\frac{\sigma_{\omega_{g-2}}}{\omega_{g-2}} = 2 \text{ ppm} .$$

The relative error in  $(g-2)$  from the mean field is  $\sigma_a/a = 13 \text{ ppm}$ . The stored intensity will be of 260 muons per  $5 \times 10^{10}$  protons of 20 GeV/c momentum and a pion beam flux injected in the storage ring of  $6 \times 10^5$  pions. The momentum of the stored muons will be  $p_{\mu} = 3.88 \text{ GeV/c}$  with  $(\Delta p/p)_{\mu} \simeq \pm 1\%$ . The running time to collect  $10^8$  decay electrons with energy greater than  $\frac{1}{2} E_{\text{max}}$  will be  $\sim 9$  weeks. Figure 7 shows the trapping efficiency versus the  $\Delta p/p$  of the pions, and Fig. 8 shows the momentum spectrum of the stored muons.

In Table 5 we summarize the given accuracies:

Table 5

$N = 10^8$  analysed decay electrons ( $E > \frac{1}{2} E_{\text{max}}$ )  $A \sim 0.30$

Superconducting storage ring		10 m diameter iron ring	
$\epsilon_{\frac{\omega}{B}}$	$\epsilon_{\omega_{g-2}}$	$\epsilon_{\frac{\omega}{B}}$	$\epsilon_{\omega_{g-2}}$
13 ppm	2 ppm	1.6 ppm	8 ppm
Intensity of stored muons per radio-frequency 260		Intensity of stored muons per radio-frequency 610	

## 9. FINAL REMARKS

- a) From the foregoing considerations we conclude that in a new  $(g-2)$  experiment we can measure the anomalous magnetic moment to a precision of 20 ppm.
- b) The more convenient solution would seem to be to construct an iron storage ring of 10 m diameter. In such a ring the mean radius determination has been optimized.

- c) We will have to make a further study in order to optimize all the parameters involved in the project. Detailed calculations of the particle orbits, resonances, stored intensity, longitudinal polarization of the muon beam, etc., have to be done.
- d) We have also to evaluate in more detail the possible source of errors and corrections to the level of 20 ppm to the value of  $g-2/2$ . Preliminary error analysis at a level of 20 ppm shows that such a fantastic precision can be reached.
- e) We are now studying other possible schemes for determining the average magnetic field as seen by the muon beam.
- f) The superconducting storage ring seems capable of meeting all the severe requirements imposed by the  $(g-2)$  experiment. However, this unconventional solution requires considerably more technical development.

APPENDIX I

APPROXIMATE CALCULATION OF THE CAPTURED MUONS

In order to estimate rapidly the number of captured muons, it is sufficient to trace and compare in the phase space (both in the horizontal and in the vertical planes) the regions of existence of the pions and of the muons of different momenta.

Actually, in a weak focusing field, the trajectory of any particle can be represented in the phase space (with an appropriate choice of scale factors) as a circle, the centre of which in the horizontal plane is the radial position of the equilibrium orbit, and in the vertical plane is the vertical position of the median plane. One complete revolution along one of these wires corresponds to a complete betatron oscillation in the focusing ring. Taking into account the dependence of the equilibrium orbits from the momentum and the geometrical limits of the chambers, the regions of existence of the captured muons are simply limited by circles tangent to the given limits. The probability for a pion to produce a captured muon of given momentum is then evaluated by timing its trajectory (which is again a circle centred around the pion equilibrium orbit, inside or outside the chamber), and measuring which fraction of it is crossing the region of existence of the chosen muons.

A correction to take into account the decay angle between muon and pion is necessary when this angle is not small in comparison with the angular acceptance of the ring.

This method is easy to apply, and has reliable results when a beam of pions with well-defined phase space (that is, momenta spectrum and angular and spacial distribution) is injected in the ring through an injector in such a way that all the pions will accomplish nearly one revolution along the ring before being lost by hitting against the injection channel. The ratio between the length of the ring and the decay length of the pions then gives a first probability factor; then, in the phase state, the fraction of the area covered during their revolution by pions of a given momentum and of a given angular spread, and common to the existence area of muons of any chosen momentum, is easily estimated.

This operation should be repeated for several muon momenta and then repeated again for several pion momenta; it is thus possible to evaluate the capture probability of muons as a function of the pion momenta, and furthermore for a given momentum spectrum of the pions in order to evaluate the muon momentum spectrum, that is the muon distribution across the ring.

When the protons are hitting a target inside the ring the method is somewhat longer, since the momentum range and the angular spread of the pions producing captured muons are very large, and the length of the pion trajectory inside the ring is dependent on the initial conditions. The trapping efficiency must then be evaluated for many different cases; the results are nevertheless reliable enough also in this case, and it is even possible to estimate to a certain extent the degree of polarization of the captured muons.

We give below a résumé of some of the basic data and formula used:

For the ring:

Betatron wavelength:

$$\lambda_H = 2\pi\rho(1-n)^{-1/2} \simeq \frac{2\pi}{0.3 B} p(1-n)^{-1/2} \begin{pmatrix} p \text{ in GeV/c} \\ B \text{ in Wb/m}^2 \end{pmatrix}$$

$$\lambda_V = 2\pi\rho n^{-1/2} \simeq \frac{2\pi}{0.3 B} p n^{-1/2} .$$

Equilibrium orbit:

$$\frac{\Delta\rho}{\rho_0} = \frac{\Delta p}{p_0} (1-n)^{-1} .$$

Angular acceptance of the ring:

$$\dot{x}_{\max} = \pm b (\lambda_H/2\pi)^{-1}$$

$$\dot{y}_{\max} = \pm a (\lambda_V/2\pi)^{-1}$$

b and a being the semiaperture, horizontal and vertical, of the chamber.

For the kinematics of  $\pi$ - $\mu$  decay:

$$p^* \approx 30 \text{ MeV}/c$$

$$\text{pion mass} = 139.6 \text{ MeV}$$

$$\text{muon mass} = 105.6 \text{ MeV}$$

$$p_\mu \approx p_\pi (0.79 + 0.21 \cos \vartheta^*) .$$

The decay distribution being isotropic in the centre-of-mass of the pions, the probability of decay is constant in function of  $\cos \vartheta^*$ , and the differential momentum spectrum of the muon is flat. The probability of decay inside the momentum bite  $\Delta p_\mu$  is then:

$$f_{\Delta p} = \frac{\Delta p_\mu}{0.42 p_\pi} \quad \text{for } 0.58 p_\pi \leq p_\mu \leq p_\pi$$

(otherwise  $f_{\Delta p} = 0$ )

The longitudinal polarization of the muon in the centre-of-mass is about equal to  $\cos \vartheta^*$ .

NEW MULTI-CHANNEL DIGITAL TIME RECORDER (DIGITRON)

I. Pizer

Here are some considerations for a new design. The following data is used as a starting point.

- (1) 200 MHz clock. Later, 256 MHz may be more convenient. If a higher frequency is requested (say 400 MHz) some (undefined) amount of development will be required to obtain full reliability and certainty, and will have a minor effect on the logic design (extra storage bit per word).
- (2) An average of 880 stops (decay electrons) per muon storage cycle. This suggests a buffer size of 1024 words. These stops occur over 300  $\mu$ sec.
- (3) Average stop rate at beginning is 20 per  $\mu$ sec, reducing to less than 1/ $\mu$ sec near 300  $\mu$ sec, with a maximum likely stop-spacing of 50  $\mu$ sec.
- (4) Since many detectors will be used, splitting of the digitron into many smaller digitrons should be envisaged.

GENERAL REMARKS

The present Digitron system using one scaler per decay electron for up to 60 decays per storage cycle seems hardly practical for the expected 880 decays in the new experiment; therefore other possible systems have been envisaged. Of these, the system whereby two or more blocks of scalers are used alternately or cyclically seem the most practical.

As in the present Digitron, the clocks and derandomized "Stop" signals (decay electrons) are distributed to each scaler. Each scaler counts clock pulses from the moment it starts until it is stopped by the appropriate "Stop" pulse. Stop pulses are only operative in a channel when the previous scaler has stopped and has provided an "Enable" signal -- thus the stop signals stop each scaler in sequence.

Considering the case of two blocks of scalars, the envisaged system sends clocks and stops to the first block. At some instant (see later) this activity is switched to the second block of scalars while the numbers now stored in the first block are transferred to a buffer store. This alternating action continues until the end of the muon storage cycle.

In the present Digitron, the clocks and stops are distributed serially to each scaler in sequence with small delays (about 1 nsec) between each unit. In the case of Design Nos. 1 and 3 below, this can also be done. In Design No. 2 we must use a parallel or "fan-out" distribution of clock and stop pulses to each scaler.

The final design depends greatly on the speed of the buffer store. The total cost depends on the number of scalars required and the size of the buffer. Various alternative solutions are discussed below.

#### Design No. 1

The blocks of scalars are switched at fixed time-intervals. To fix our ideas let us assume a 200 MHz clock, a 1  $\mu$ sec time slot (switch between blocks of scalars each 1  $\mu$ sec), and 32 scalars in each block. Since there are 200 clocks in 1  $\mu$ sec, our scalars will need 8 bits. Since we also expect to average 20 stops per  $\mu$ sec at the beginning, we will usually have some scalars not receiving stops, so they will stop counting on the last clock pulse. We will not be able to distinguish a valid stop on the last clock pulse from a non-stopped scaler unless we use a tag-bit operated by the "Enable" signal of the appropriate scaler. So we need to transfer 9 bits of information to the buffer\*).

We must transfer blocks of scaler numbers to the buffer over a period of 300  $\mu$ sec so we must transfer  $300 \times 32 = 9600$  words of 9 bits -- this dictates the size of our buffer.

The above example was somewhat arbitrary -- let us see what happens when we vary the width of the time slot, using a 200 MHz clock.

---

\*) The extra bit per word could be suppressed if one extra clock pulse is injected at the end of each time-slot.



Time slot	No. of clocks	Scalers/block	Bits/scalers	Bits to buffer	No. of blocks	Buffer words	Total bits	Buffer bits/ $\mu$ sec
4 $\mu$ sec	800	128	10	11	75	9600	105.600	352
2 $\mu$ sec	400	64	9	10	150	9600	96.000	320
1 $\mu$ sec	200	32	8	9	300	9600	86.400	288
$\frac{1}{2}$ $\mu$ sec	100	16	7	8	600	9600	76.800	256
$\frac{1}{4}$ $\mu$ sec	50	8	6	7	1200	9600	67.200	224
160 nsec	32	5	5	6	1875	9375	56.250	190

The shorter slot requires less scalers with less bits per scaler and slower transfer rate of bits to the buffer. It does not offer greater difficulties to the designer of the fast switching circuits, since in any case they must operate at speeds determined by the spacing between clock pulses.

The problem of the buffer has not yet been raised. With a  $\frac{1}{2}$   $\mu$ sec slot we must transfer 128 bits in  $\frac{1}{2}$   $\mu$ sec. If we can use a buffer with an input word of 64 bits, we need to write a 64-bit word each 250 nsec. This is probably within the present state of the art for fast-core or thin-film memories. We therefore transfer 8 scaler words simultaneously to the buffer.

A single counting error in one scaler gives a single false decay measurement which may in any case be detectable if the number is not in sequence. The error is not cumulative. A repeated error in one scaler should be program detectable.

An error in the time-slot scaler would be disastrous. By duplicating this scaler it will be possible to give an alarm should the two scalers not remain in exact synchronism.

An interesting variation is to consider a clock frequency of 256 MHz. With a  $\frac{1}{2}$   $\mu$ sec slot, the number of clocks becomes 128, giving maximum utilization of scalers and making the highest number 127, i.e. all one's in the scaler bits.

The buffer size may be diminished by widening the time slot at known instants as the decay rate decreases over the muon storage time.

For example, if the slot-width is doubled each time the average stop rate decreases by a factor of 2, giving three different slot widths, the buffer size can be reduced to less than 40% words. However, the word size must increase by 2 bits unless the clock rate can also be decreased by a factor of 2 at the same instant.

### Design No. 2

Switch to next block of scalars when all scalars stopped. This means we transfer only valid words to the buffer and, in principle, need a buffer with as many words as expected stops, say 1024 words.

However, in this case our scalars need more bits, since any one scalar may be called upon to count clocks at least over the maximum spacing between stops (say 50  $\mu$ sec), so a scalar needs 14 or 15 bits -- let us say 15.

Since we transfer only valid words and in groups equal in size to the block size, we do not need to include a flag bit. At the end of a measurement we will probably have a partly filled block of scalars -- this block must also be transferred. Scalars which had not been stopped by "Stop" pulses will have identical numbers. We will not be able to distinguish whether or not there was one valid "Stop" at this last number, but we can probably ignore this eventually.

An error in the last scalar of a block accumulates in all subsequent time measurements, since we do not have a fixed time-slot. We can take out an insurance policy against this by duplicating the last scalar in a block and always requiring identical numbers in the duplicated scalars, though we need not transfer the duplicate value into the buffer.

A variable number of words are transferred to the buffer at each muon storage cycle. This number will be known (buffer address register) and could be used to transfer to the computer only the useful buffer words. However, it will probably be less complicated to transfer always the full buffer and let the computer program sort out valid words.

Because of the larger word size, we need a greater bit transfer rate to the buffer than in Design No. 1.

Possible variation on

Scalers/block	Bits/scaler	Av. time to fill block	No. of blocks
128	15	6.4 $\mu$ sec	8
64	15	3.2 $\mu$ sec	16
32	15	1.6 $\mu$ sec	32
16	15	0.8 $\mu$ sec	64
8	15	0.4 $\mu$ sec	128
4	15	0.2 $\mu$ sec	256

The maximum word transfer rate remains about the same for all cases at 32 words/ $\mu$ sec = 512 bits/ $\mu$ sec. This is about twice the rate required in Design No. 1 -- feasibility will depend on available buffers or parallel running of smaller, slower buffers.

The only advantage in using more scalers in a block is the decreased chance of filling a block in a time shorter than is available to empty them into the buffer.

The buffer size will remain the same for all block sizes at about 1024 words to accommodate the average of 880 stops.

Switching clock and stop pulses from one block to another poses the following timing problem. The switching must take place between one clock pulse and the next -- this means that the delay between the clock switching gate and back to the gate must be well below the interval between the operative stop and the next clock. Considerable care in the physical disposition of these circuits will therefore be necessary.

### Design No. 3

Fixed time-slot but only transfer valid words.

This is a composite of the previous two designs. Scalers need only have sufficient bits to cover the time-slot. However, now we do not know to which time-slot the numbers belong, so we must invent a tagging system of some sort. Since a time-slot may contain no valid stops, we probably

need a tag word every time-slot. This word could be a count of time-slots. Since we must also be able to distinguish this word from the time measurement, we also need a tag-bit. Various possibilities are as follows:

Time-slot	Bits/scaler	Bits in buffer word	Scalers per block	Buffer words	n
4 $\mu$ sec	10	11	128	1024+ 75+n	200
2 $\mu$ sec	9	10	64	1024+ 150 +n	450
1 $\mu$ sec	8	9	32	1024+ 300 +n	1050
$\frac{1}{2}$ $\mu$ sec	7	8	16	1024+ 600 +n	2400
$\frac{1}{4}$ $\mu$ sec	6	7	8	1024+1200+n	4800
160 nsec	5	6	5	1024+1875+n	9000

The number of buffer words is increased by two effects: the first is the time-slot count word occurring at every block transfer; the second is the value n, which is caused by the fact that one must send several words in parallel to the buffer [this means that some invalid words are transferred, recognized from the tag-bit]. If W words are transferred in parallel, then an average of W/2 invalid words are transferred per time slot  $\tau/\mu$ sec; therefore

$$n = \frac{300}{\tau} = \frac{W}{2} .$$

The value of n is tabulated for a transfer of 64 bits in parallel.

#### The buffer

Only very general considerations have been given so far. Various types of memories (ferrite-core, thin-film, micrologic scratch-pad) are possible, and cover a wide range of prices. Due to the high rate of data transfer into the buffer, we need to transfer several words in parallel (into a single memory, or several separate memories simultaneously).

The micrologic solution gives a very high cost, but also great speed. The market will be searched to find suitable memories.

### Clocks and Stops

The basic problems of switching speeds, etc., will be similar to the present design, but the organization will differ according to the chosen system. We will write something more detailed at a later date, discussing these problems.

### Splitting the Digitron

#### Design No. 1:

Provided the clock pulses are suitably distributed and the stops processed separately for each digitron section, the scalers in the blocks can be split into sections and can be utilized separately. The computer will receive the various numbers, somewhat interleaved, but in a known pattern. The number of mini-Digitrons depends on the number of scalers provided in each block.

If there were 24 scalers per block divided amongst 24 detectors, only one stop could be recorded per time-slot per Digitron. This is an argument for either increasing the number of scalers per block or decreasing the requirement (only asking for 6 mini-Digitrons and 30 scalers per block, giving 5 scalers per block per mini-Digitron).

#### Design No. 2:

This is somewhat more difficult to do because of the loop time-delay from the clock and stop routing gate, through the scaler inputs to the final "Enable" signal which must actuate the clock and stop routing. Each splitting of the Digitron requires repeating these loops, in each case respecting the minimum time-delay. This may be a formidable task of miniaturization.

#### Design No. 3:

The problem on the scaler input side is similar to that for Design No. 1. On the buffer transfer side, scalers to be transferred will be interspersed with some scalers not to be transferred, thus giving a different requirement than for the single digitron case. Any advantage over Design No. 1 will probably be lost in the complex statistical situation.

SUMMARY

There appear to be more advantages in Design No. 1, and less complexities than in the other possibilities. More thinking about details, and especially more information on memories, is needed before a final decision can be made. The exact requirement for splitting into several mini-Digitrons will influence the decision.

REFERENCES

- 1) F.J.M. Farley, J. Bailey, R.C.A. Brown, M. Giesch, H. Jöstlein, S. van der Meer, E. Picasso and M. Tannenbaum, Nuovo Cimento 45, 281 (1966).
- 2) J. Bailey, W. Bartl, R.C.A. Brown, F.J.M. Farley, H. Jöstlein, S. van der Meer and E. Picasso, "The anomalous magnetic moment of the  $\mu^-$ ", Proc.Int. Symposium on Electron/Photon Interactions at High Energy, Stanford (1967) (in press).
- 3) R.R. Williams, "On a new (g-2) experiment", CERN NP Internal Report 68-8, 29.2.68.
- 4) H. Brechna et al., "A Superconducting Muon Storage Ring", CERN NP Internal Report (in preparation).
- 5) T. Kinoshita, Nuovo Cimento 51B, 140 (1967) (more detailed bibliography is given here);  
T. Kinoshita, "The anomalous magnetic moment of the muon", Lecture given at the Summer School of Theoretical Physics, Cargèse, July 1967.
- 6) Y.F. Orlov, "The stabilization of the mean muon orbits in the (g-2) experiments" (to be published in Nuovo Cimento).
- 7) A. Schoch, "Theory of linear and non-linear perturbations of betatron oscillations in alternating gradient synchrotrons", CERN 57-21 (1957).
- 8) R. Hagedorn, "Stability and amplitude ranges of two-dimensional non-linear oscillations with periodical Hamiltonian", CERN 57-1 (1957).
- 9) G.K. Green and E.D. Courant, "The Proton Synchrotron", Handbuch der Physik, Vol. XLIV (1959).
- 10) G. Charpak, F.J.M. Farley, R.L. Garwin, T. Muller, J.C. Sens and A. Zichichi, Nuovo Cimento 37, 1241 (1965).

Figure captions:

Fig. 1 : Beam layout.

Fig. 2 : Beam optics.

Fig. 3 : Injection channel (cross-section and layout).

Fig. 4 : Diagram of resonances.

Fig. 5 : The trapping efficiency versus the  $\Delta p/p$  of the pions.

Fig. 6 : The muon distribution versus equilibrium radii.

Fig. 7 : The trapping efficiency versus the  $\Delta p/p$  of the pions in the case of the superconducting muon storage ring.

Fig. 8 : The muon distribution as a function of the  $\Delta p/p$  of the stored muons in the case of the superconducting storage ring.



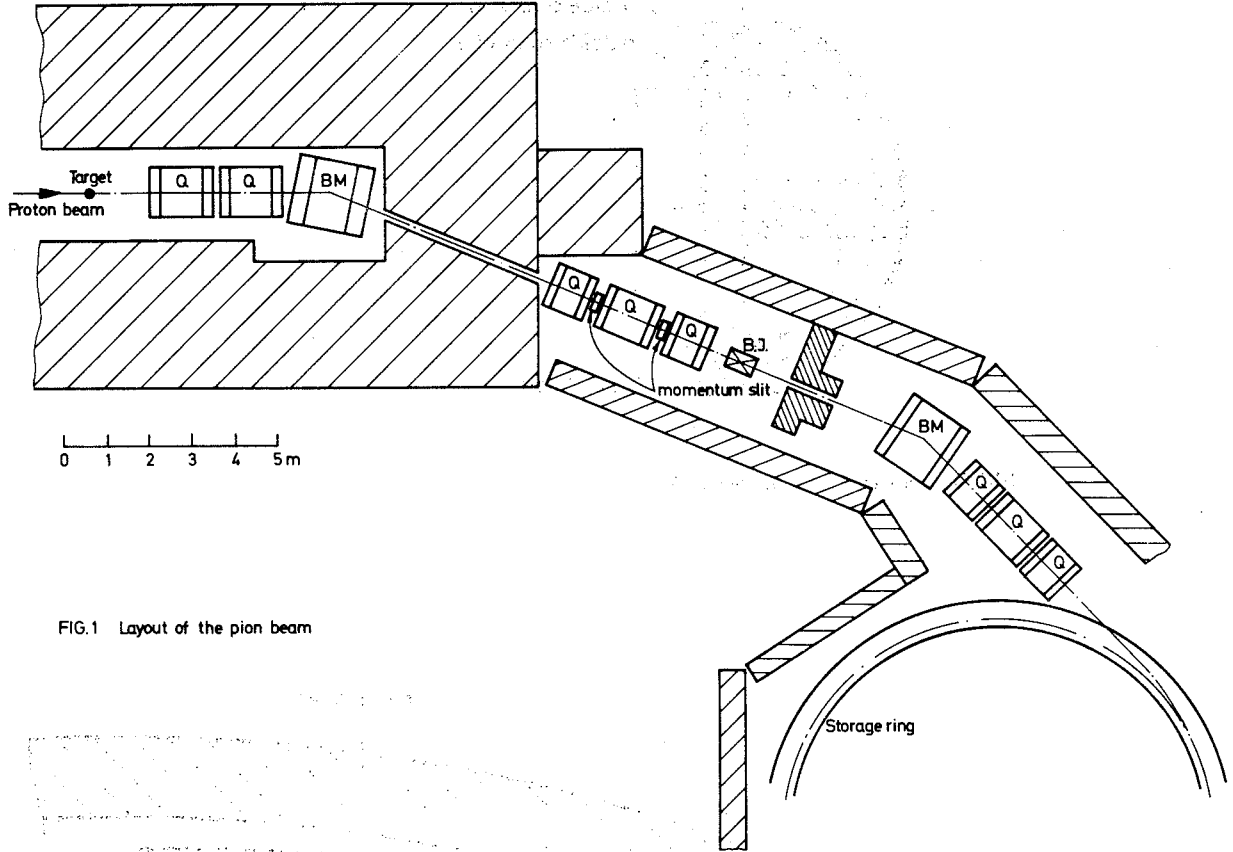


FIG.1 Layout of the pion beam

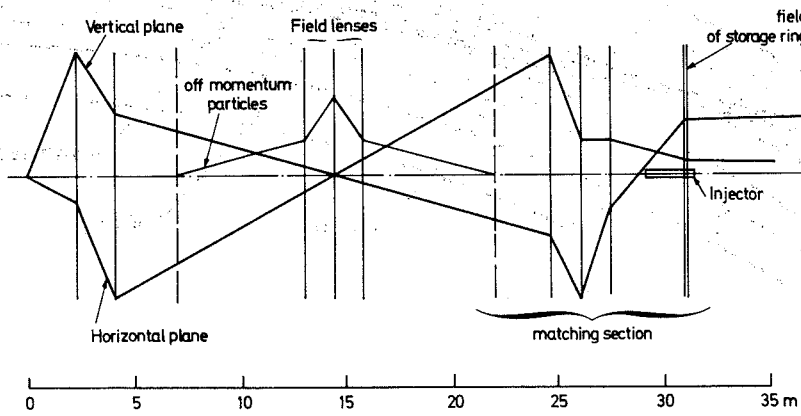


FIG.2 Optical behaviour of the pion beam

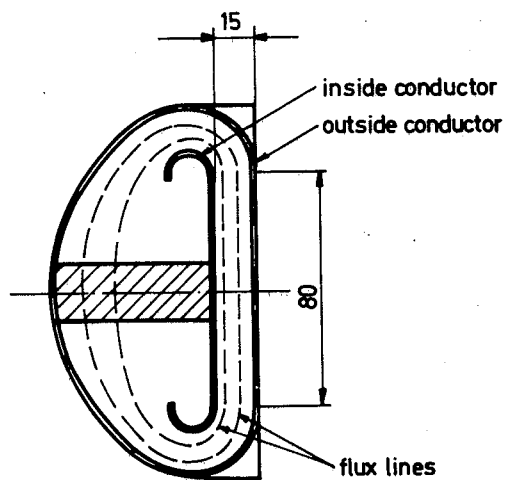


FIG. 3a Inflector cross-section

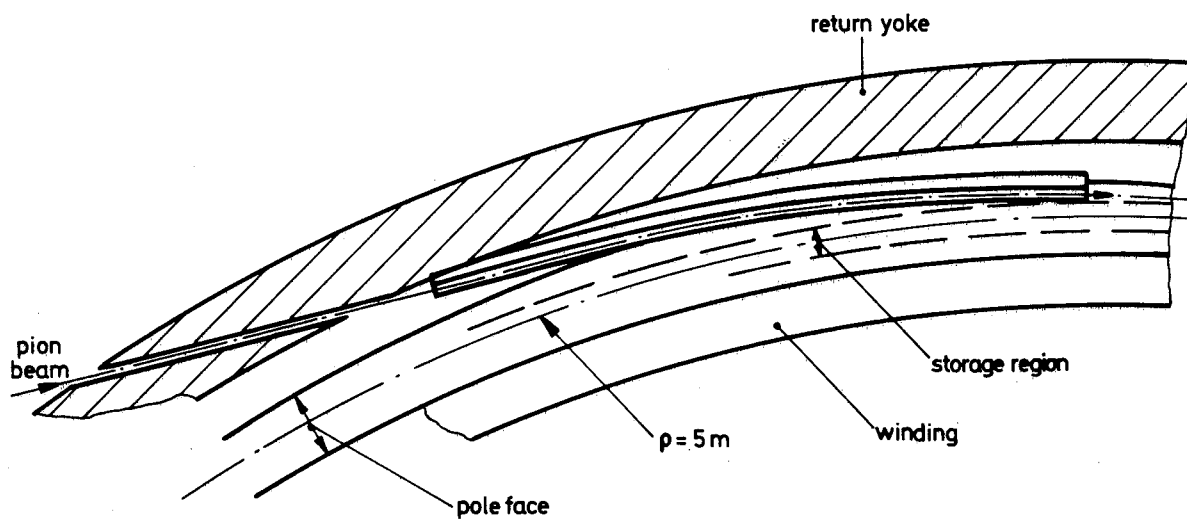


FIG. 3b Location of the inflector in the 10m  $\phi$  ring

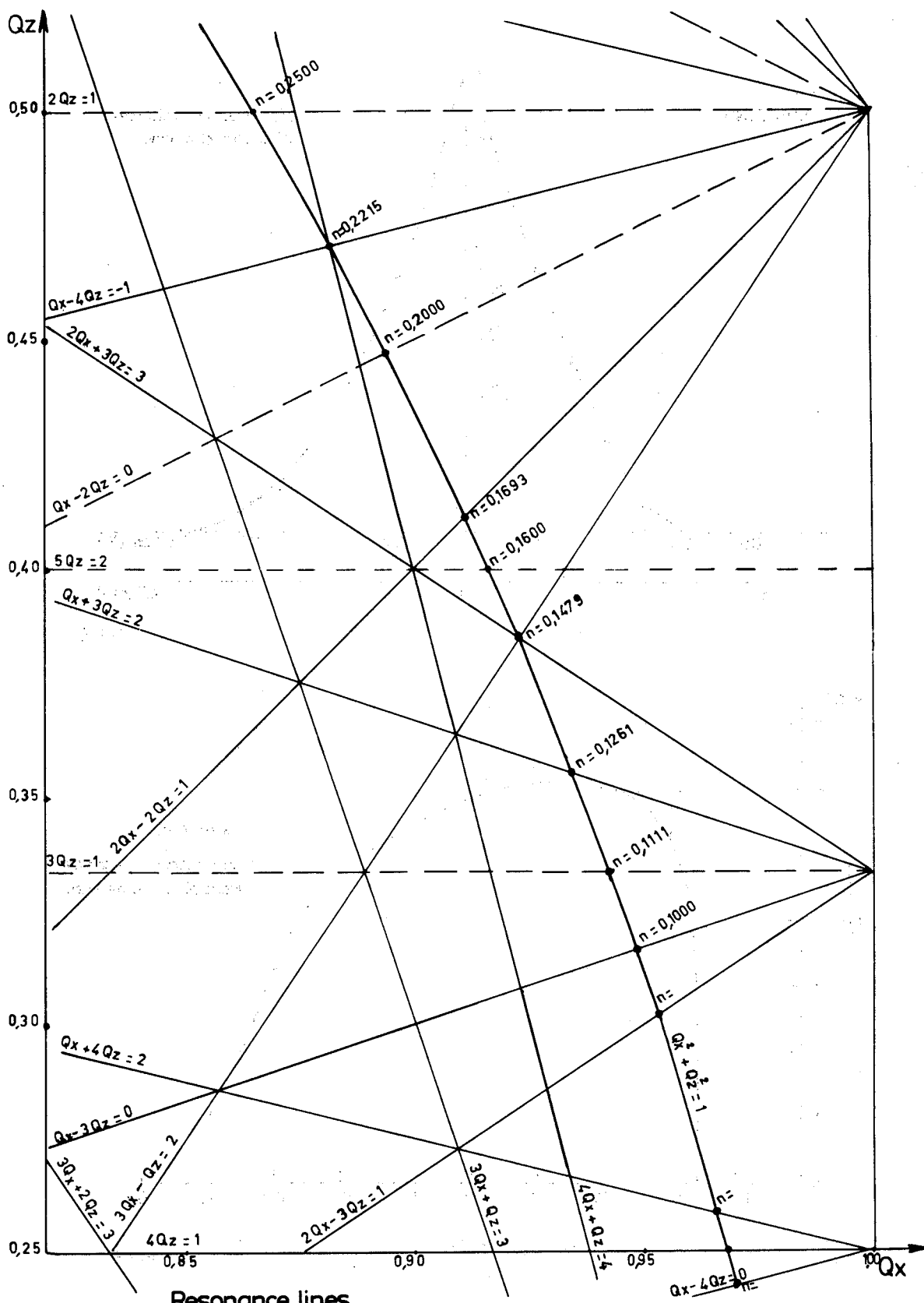


FIG.4

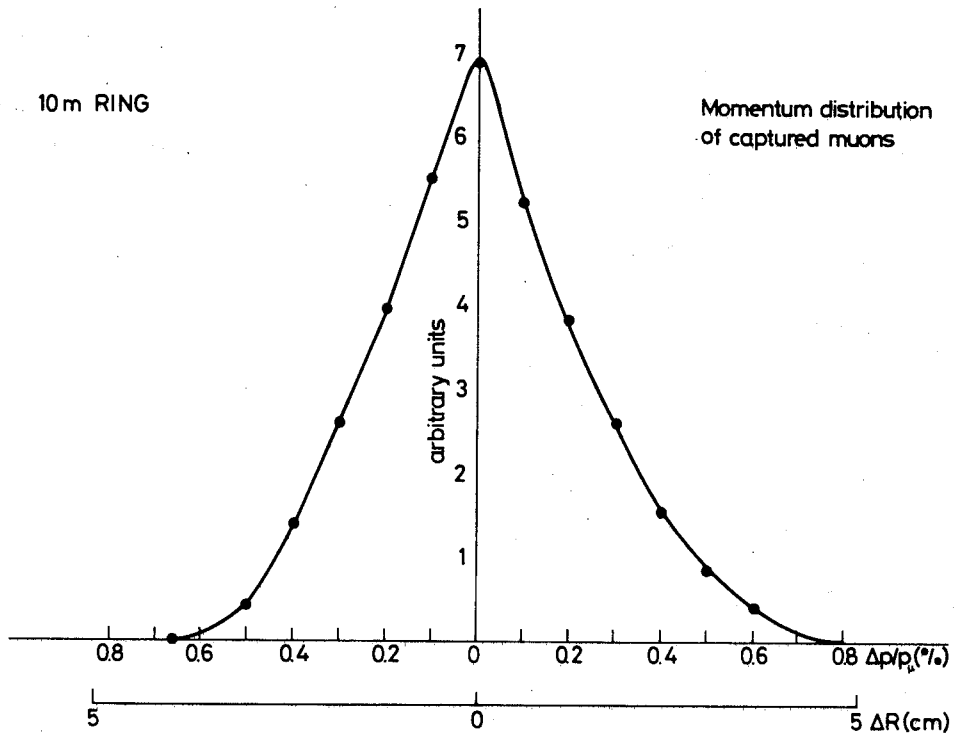


FIG. 5

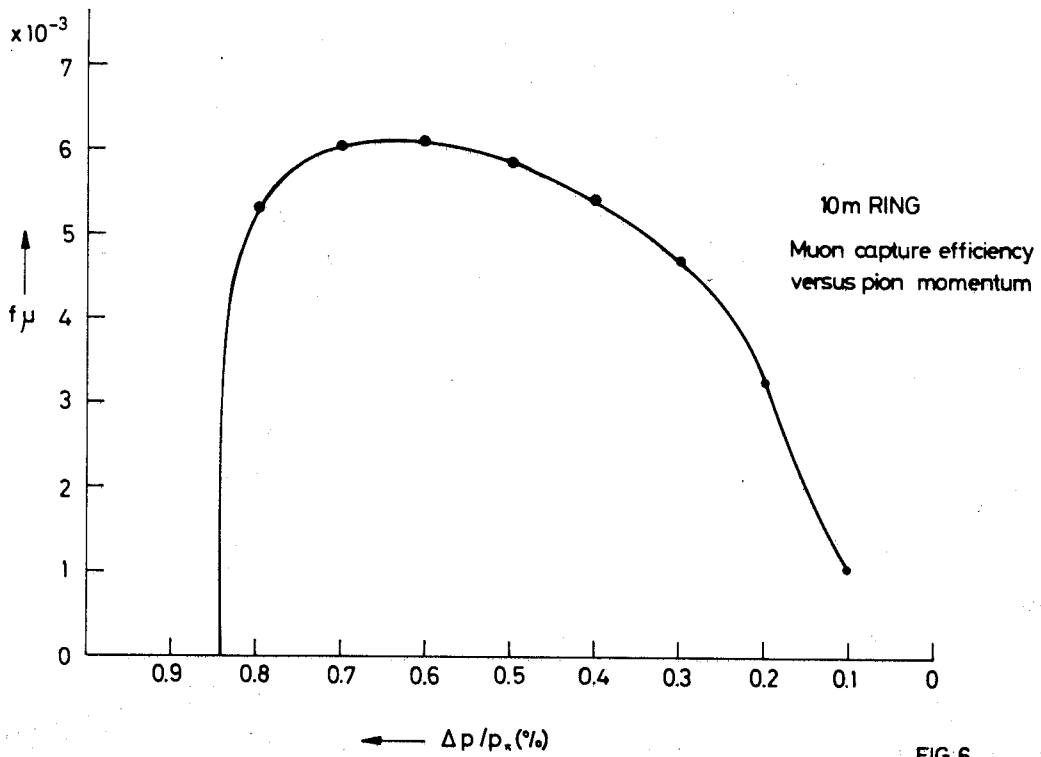


FIG. 6

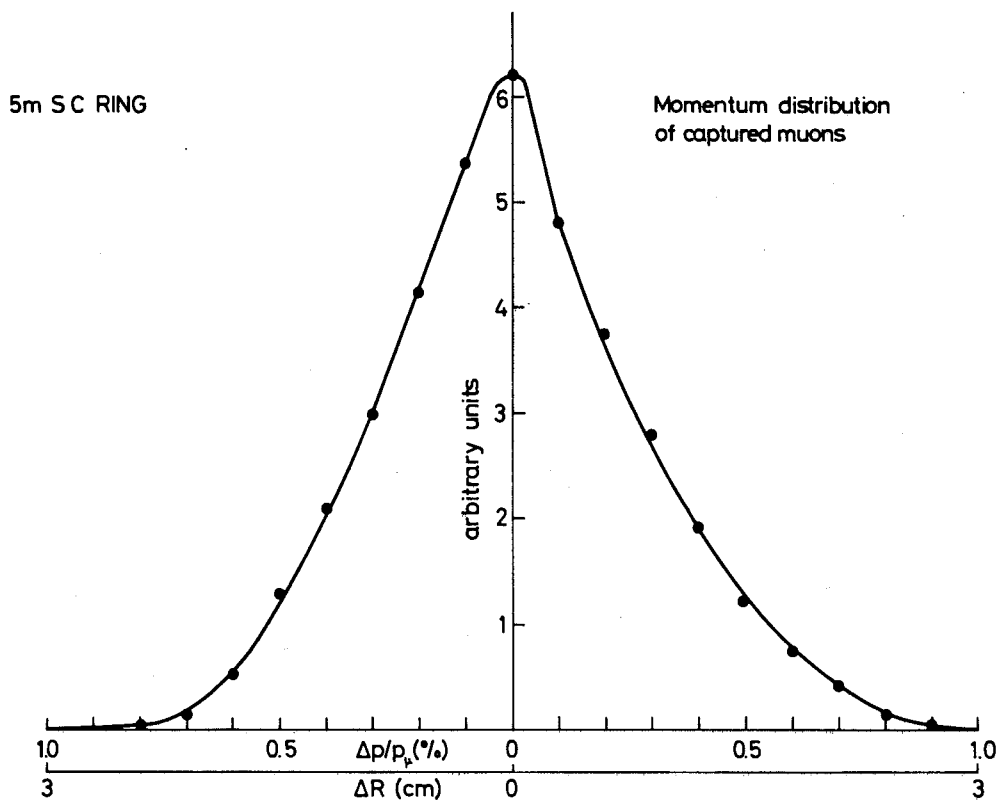


FIG. 7

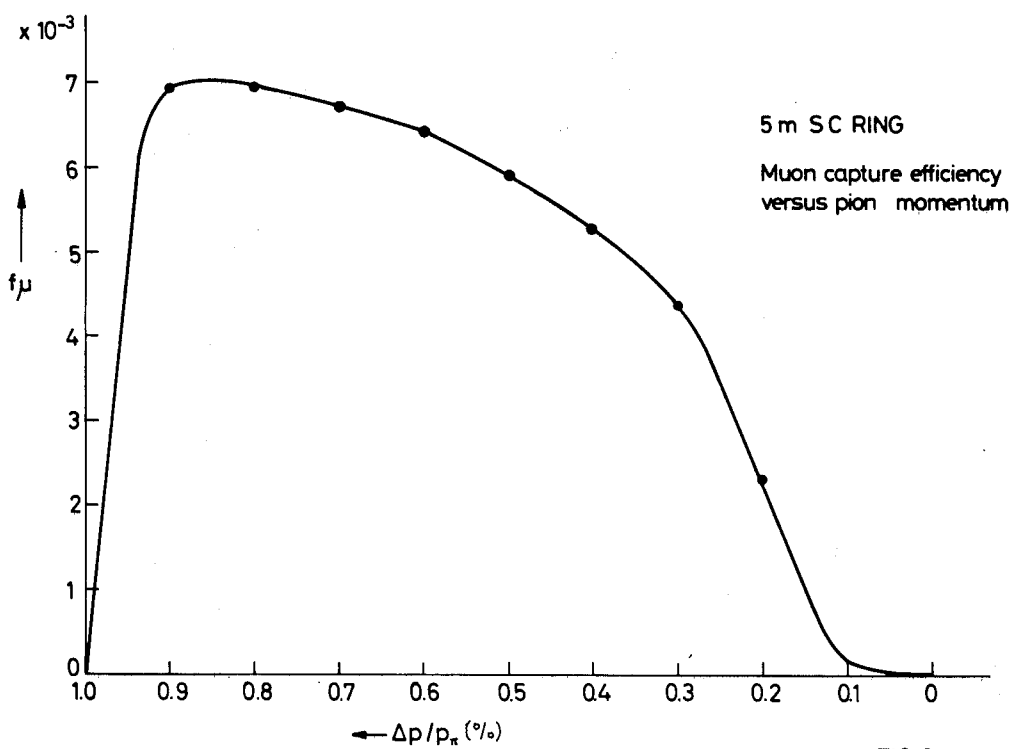


FIG. 8